Single-Stranded DNA: Replacement of Canonical by Base-Modified Nucleosides in the Minihairpin 5′-d(GCGAAGC)-3′ and Constructs with the Aptamer 5′-d(GGTTGGTGTGGTTGG)-3′[1])

by **Helmut Rosemeyer**, **Verena Mokrosch**, **Anup Jawalekar**, **Eva-Maria Becker**, and **Frank Seela***[2])

Laboratorium für Organische und Bioorganische Chemie, Institut für Chemie, Universität Osnabrück, Barbarastr. 7, D-49069 Osnabrück
(phone: 0049-541-9692791; fax: 0049-541-9692370; e-mail: frank.seela@uni-osnabrueck.de)

Dedicated to the memory of the late Prof. Dr. *Friedrich Cramer*, Göttingen

The minihairpin 5′-d(GCGAAGC)-3′ (**1**) was modified either in the loop region, in the base-paired stem, or at the 5′-terminus by incorporation of base-modified nucleosides. The thermal melting was correlated to the structural changes induced by the various donor-acceptor properties of the nucleosides. Overhanging nonpaired nucleosides at the 5′-terminus stabilized the hairpin, while a reverse of the $dG^3 \cdot dA^5$ sheared base pair to $dA^3 \cdot dG^5$ severely affected the stability. The combination of the minihairpin 5′-d(GCGAAGC)-3′ (**1**) and the thrombin-binding aptamer 5′-d(GGTTGGTGTGGTTGG)-3′ (**2** (=**46**)) resulted in the new construct 5′-d(GGTTGGGCGAAGCGGTTGG)-3′ (**43**) arising by replacement of the 5′-d(TGT)-3′ loop of **2** by the minihairpin. The fused oligonucleotide **43** exhibits a two-phase thermal transition indicating the presence of the two unaltered moieties. According to slight changes of the T_m values of the construct **43** as compared to the separate units **1** and **2**, cooperative distorsions are discussed.

Introduction. – Short single-stranded nucleic acids are valuable structural tools in the bottom-up strategy of nanotechnology [1]. Usually, a single-stranded DNA forms already an ordered helical structure which results from base stacking and the restricted conformation of the single bonds in the sugar moiety [2]. Due to a particular base sequence, single-stranded DNA can be transformed into a hairpin which is built up from a base-paired stem and a non-base-paired loop region [3]. Such hairpins play an important role in the structural variation of canonical nucleic acid secondary structures and may contain unusual base pairs such as guanine · adenine pairs. Mostly mRNA, tRNAs, ribozymes, RNA aptamers, and ribonucleoproteins are known to form such motifs [4], while dG · dA-containing hairpins formed by single stranded DNA are rare [5].

Earlier, it has been observed that hairpin formation hampers the *Sanger* dideoxysequencing of DNA due to band compressions. Relief is brought about by using 7-deazapurine moieties, which cause the opening of the base-paired region of the hairpin [6]. On the other hand, hairpin formation can be successfully used for the protection of oligonucleotides, *e.g.*, of antisense or antigene oligomers against the action of nucleases: pasting, *e.g.*, the minihairpin-forming oligonucleotide **1** (*Fig. 1,a*)

---

[1]) Parts of this work are published in the Diploma Thesis of *V. M.*, University of Osnabrück, 2000.

[2]) In cooperation with the *Center for Nanotechnology* (*CeNTech*), Gievenbecker Weg 11, D-48149 Münster.

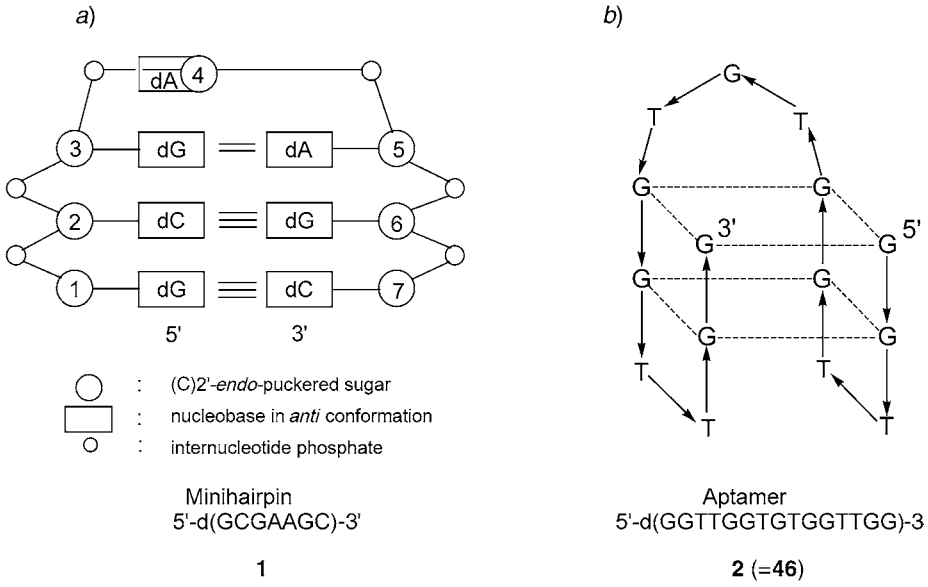

Fig. 1. *Schematic presentation of* a) *the minihairpin 5′-d(GCGAAGC)-3′* (**1**) *as well as of* b) *the thrombin-binding aptamer* **2** (=**46**) *adopting a monomer chair built-up from a G quartet*

to the 3′-end of an antisense oligonucleotide endows the latter with stability towards enzymatic exonucleolytic digestion.

Multiple nucleic acid hairpins are found in guanosine-rich oligonucleotides having the propensity to form quadruplex structures stabilized by G quartets. There is a considerable interest in the therapeutic potential of such quadruplexes, particularly in aptamers or non-antisense antiproliferative agents [8]. Intramolecular fold-back structures with a G-quartet motif such as the thrombin-binding aptamer **2** (*Fig. 1,b*) [9] can be looked upon as a triple minihairpin containing two two-nucleotide and one three-nucleotide loops and exhibiting also a significant thermal stability (T_m 48°).

We now report on the incorporation of the modified nucleosides **4**–**6**, **9**, and **10** as well as of the abasic compounds **7** and **8** into different positions of the minihairpin 5′-d($G^1C^2G^3A^4A^5G^6C^7$)-3′ (**1**) and investigate the influence of the modified residues on the hairpin stability. Also, the thermal stabilization of the minihairpin will be studied by using various 5′-dangling nucleosides. By this way, *i*) the particular structure of the sheared $dG^3 \cdot dA^5$ base pair (*Fig. 1,a*) will be corroborated, and *ii*) the possibility of a stability adjustment of the minihairpin **1** will be plumbed. Additionally, a construct consisting of the hairpin and the thrombin-binding aptamer is prepared. Its thermal melting will be compared with that of the separate moieties, and conclusions on the structural modification of the aptamer by the minihairpin will be drawn.

2. Results and Discussion. – 2.1. *Preamble.* The heptamer 5′-d($G^1C^2G^3A^4A^5G^6C^7$)-3′ (**1**) as well as the related octamer 5′-d(GCGAAAGC)-3′ have been studied intensively because they form extraordinarily stable hairpins (T_m 72° (**1**) and 76°, resp.) [10]. The

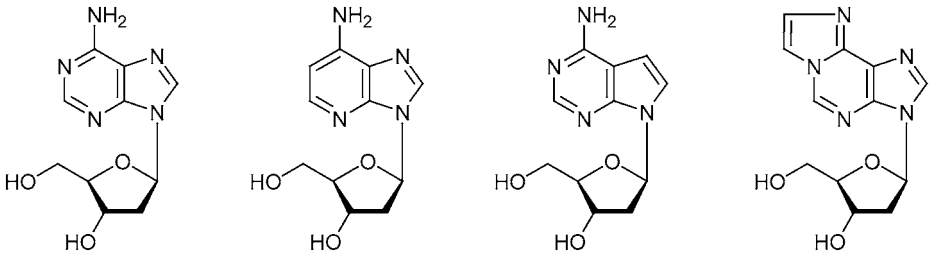

3 **4** **5** **6**

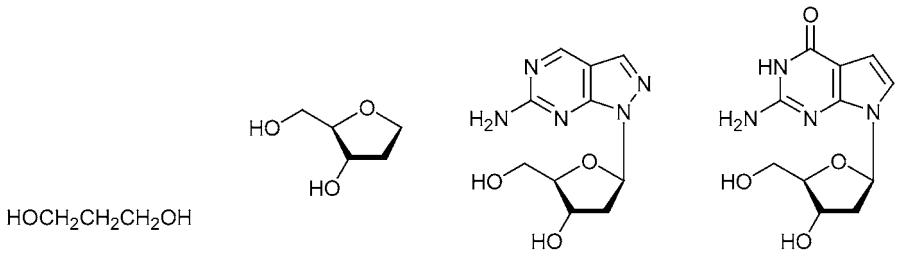

7 **8** **9** **10**

reason for this stability is the entropy of hairpin formation. Their melting profiles, however, exhibit often low cooperativity. Stacking interactions are of particular importance for the stability of such structures. Hairpin sequences such as **1** or 5′-d(GCGAAAGC)-3′ occur frequently in biologically important regions such as replication origins and promotor regions [11]. The 3D structure of both oligonucleotides, determined by NMR spectroscopy, discloses the reason for this striking property: They form unusual minihairpins, whereby the heptamer **1** contains just one dA residue within the loop. An adjacent sheared $dG^3 \cdot dA^5$ base pair (see motif **I** below) occurs at the single phosphate intervening between dA^4 and dA^5 (*Fig. 1,a*). Comparison of the geometries of this unusual pair and of the *Watson–Crick* (*W.–C.*) dG · dC base pair shows that the distance of the 3′-phosphate of dG^3 and the 5′-phosphate of dA^5 is shortened to 7.5 Å, while the distance of the equivalent phosphates of the *W.–C.* base pair amounts to 16.4 Å. This allows the formation of a one-nucleotide loop, while for regular *W.–C.* base pairs, four to five nucleotide residues in a loop are needed to build up a stable hairpin. Additionally, the $dG^3 \cdot dA^5$ pair causes strong intrastrand stacking interactions along the hairpin stem.

2.2. *Oligonucleotide Synthesis and* T_m *Measurements.* The synthesis of the various modified hairpins (see *Table 1*) was performed on solid phase with the phosphoramidites **11**–**17** and with the phosphoramidites of the regular nucleosides (→**18**–**50**). Most syntheses followed the standard protocols [12]; coupling yields of the modified phosphoramidites are given in *Table 1*. Base deprotection was performed with 25% aqueous ammonia (60°, overnight). Only the oligomers carrying 1,N^6-etheno-2′-

deoxyadenosine (**6**) or 1-deaza-2′-deoxyadenosine (**4**) were prepared with (*tert*-butyl)phenoxyacetyl-protected canonical nucleoside building blocks; in these cases, the 'fast deprotection' method was used for subsequent deprotection (see *Exper. Part*). The oligonucleotide synthesis was performed in the 'trityl-off' mode, and the oligomers were purified by reversed-phase HPLC (*RP-18*). The homogeneity was established by HPLC (*RP-18*) as well as by ion-exchange chromatography (*NucleoPac-PA-100* column, 4 × 50 mm; *Dionex*, P/N 043018, USA). The modified oligonucleotides were characterized by MALDI-TOF mass spectra. The detected masses were in good agreement with the calculated values (*Table 1*).

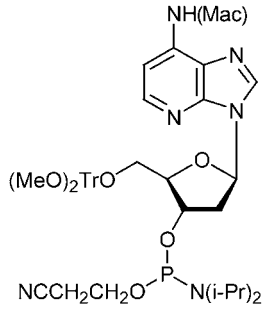

11

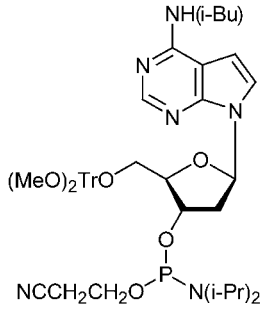

12

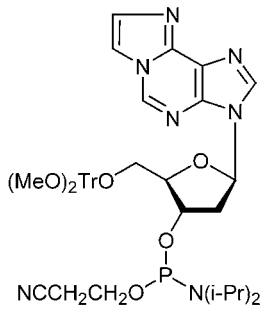

13

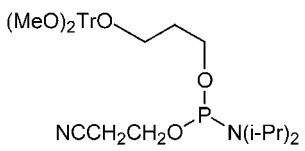

14

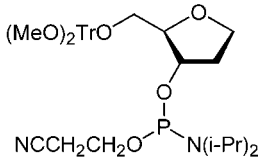

15

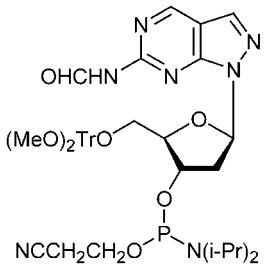

16

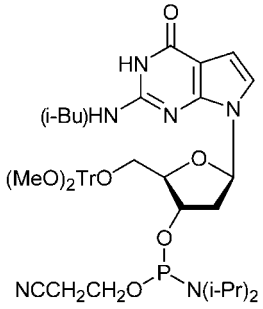

17

Table 1. *Data on Oligonucleotide Synthesis and Molecular Masses of Chemically Modified Oligomers Determined by MALDI-TOF Mass Spectra*

Oligonucleotide[a])	Coupling yield [%]	Final yield [A_{260} units]	$[M+H]^+$ [Da]	
			calc.	found
5′-d(GCGAAGC)-3′, **1**	–	12	2129	2130
5′-d(GCG**4**AGC)-3′, **21**	95	10	2128	2130
5′-d(GCGA**4**GC)-3′, **22**	95	14	2128	2129
5′-d(GCG**44**GC)-3′, **23**	97, 100	12	2127	2129
5′-d(GCG**5**AGC)-3′, **24**	98	6	2128	2128
5′-d(GCGA**5**GC)-3′, **25**	100	6	2128	2130
5′-d(GCG**55**GC)-3′, **26**	100, 98	9	2127	2129
5′-d(GCG**6**AGC)-3′, **27**	99	10	2153	2153
5′-d(GCGA**6**GC)-3′, **28**	100	9	2153	2153
5′-d(GCG**66**GC)-3′, **29**	98, 98	2	2177	2177
5′-d(GCG**7**AGC)-3′, **30**	98	8	2113	2113
5′-d(GCG**8**AGC)-3′, **31**	79	1	1954	1954
5′-d(GC**9**AAGC)-3′, **32**	100	1	1996	1997
5′-d(**A**GCGAAGC)-3′, **34**	–	5	2445	2449
5′-d(**5**GCGAAGC)-3′, **35**	98	2.5	2444	2444
5′-d(**6**GCGAAGC)-3′, **36**	95	1	2468	2471
5′-d(GC**10**AAGC)-3′, **33**	96	12	2128	2127
5′-d(GCAAGGC)-3′, **39**	–	13	2129	2130
5′-d(GGTTGGTGTGGTTGG)-3′, **2**	–		4727	4729
5′-d(GGTTGGT**10**TGGTTGG)-3′	70		4726	4726
5′-d(GGTTGGTTGGTTGG)-3′, **48**	–		4398	4398
5′-d(GGTTGGGCGAAGCGGTTGG)-3′, **43**	–		5982	5982
5′-d(GGTTGGCGAAGGGTTGG)-3′, **44**	–		5364	5362
5′-d(GGTTGGGAAGGTTGG)-3′, **45**	–		4745	4746
5′-d(GGTTTGGTGTGGTTGG)-3′, **49**	–		5031	5031
5′-d(GGTTGGTGTGGTTTGG)-3′, **50**	–		5031	5032

[a]) The underlined oligonucleotide sequence marks the modification of the corresponding parent sequence.

In the following, the temperature-dependent UV absorbance of the various oligonucleotides were measured, and their T_m values were calculated, usually as a function of different oligomer concentrations (see *Exper. Part*). In most cases, the T_m values were found to be independent of the concentration, thus establishing monomolecular-hairpin formation. Experiments performed with oligonucleotides containing either 7-deaza-2′-deoxyadenosine (**5**) or -guanosine (**10**) confirmed data reported earlier by others [10].

2.3. *Thermal Stability of the Minihairpin* **1** *Containing the Modified Nucleosides* **4**–**10**. 2.3.1. *Loop Modifications.* The hairpin **1** shows an almost identical T_m value (69–72°) in four different buffer systems (*Table 2* and *6*, *Entries 1–3* and *51*). Replacement of dA^4 forming the miniloop by the other regular nucleosides leads also to highly stable hairpin structures (*Table 2*, *Entries 4–6*), whereby purine nucleotides in position 4 exhibit slightly higher T_m values than pyrimidine nucleotides. This is due to stronger stacking interactions of the purine bases between the dG^3 residue and the loop-forming nucleoside. It had been shown by NMR analysis that the fourth nucleobase being unpaired stacks on the third one (guanine) and that a sharp turn within the loop region

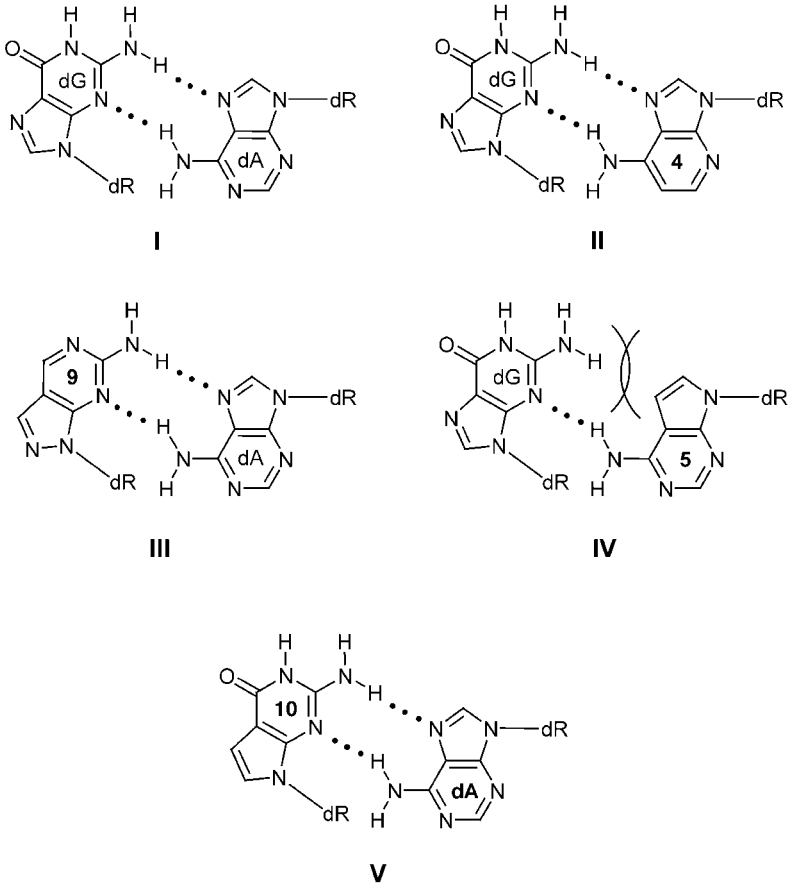

I II III IV V

occurs at the three bonds dA^4(O(3′)–P), dA^5(O(5′)–P), and dA^5(C(5′)–C(4′)). From the four different motifs that are conceivable for the $dG^3 \cdot dA^5$ base pair, motif **I** was shown to be formed by the unmodified hairpin **1**.

First, compounds **4**–**8** were incorporated into position 4 of the hairpin **1** instead of dA^4. As can be seen from *Table 2* (*Entries 7–16*), the replacement of dA^4 by 1-deaza-2′-deoxyadenosine (**4**; c^1A_d) leads only to a slight decrease of the T_m value ($\Delta T_m = -(1-3^\circ)$, depending on the oligomer concentration and the buffer used). This reflects the similar polarizability of the 1-deazaadenine base compared to that of adenine ($\alpha_m(c^1\text{Ade}) = 15.43 \pm 0.5 \cdot 10^{-24}$ cm^3; $\alpha_m(\text{Ade}) = 14.68 \pm 0.5 \cdot 10^{-24}$ cm^3)[3]). Also the introduction of 7-deaza-2′-deoxyadenosine (**5**; c^7A_d) and even of the tricyclic 1,N^6-etheno-2′-deoxyadenosine (**6**; εA_d) does not alter the T_m value of the parent oligomer

[3]) Molecular polarizability values were calculated from polarizability increments (central atom and neighboring sphere considering the order and aromaticity of bonds) by using the program ChemSketch [13] (the units of polarizability α_m, given in cm^3, should strictly be $4\pi\varepsilon_0$).

significantly (*Table 2*, *Entries 17* and *20*, resp.), indicating that the stacking overlap of the forth base onto the third is not as pronounced in solution as one may deduce from the NMR structural analysis.

Table 2. T_m *Values and Thermodynamic Data of the Formation of the Parent Minihairpin* **1** *as well as of Chemically Modified Derivatives in Different Buffer Systems*

Entry	Oligonucleotide[a])	Conc. [μM]	Buffer[b])	T_m [°]	ΔH° [kcal/mol]	ΔS° [cal/(mol K)]	ΔG°_{310} [kcal/mol]
1	5′-d(GCGAAGC)-3′, **1**	10	*A*	69	−27	−79	−2.5
2	5′-d(GCGAAGC)-3′, **1**	10	*B*	69	−24	−70	−2.3
3	5′-d(GCGAAGC)-3′, **1**	10	*C*	72	−31	−89	−3.2
4	5′-d(GCGGAGC)-3′, **18**	10	*C*	71	−31	−89	−3.0
5	5′-d(GCGCAGC)-3′, **19**	10	*C*	67	−30	−90	−2.7
6	5′-d(GCGTAGC)-3′, **20**	10	*C*	66	−29	−86	−2.5
7	5′-d(GCG**4**AGC)-3′, **21**	24	*B*	66	−25	−75	−2.1
8	5′-d(GCG**4**AGC)-3′, **21**	15	*B*	67	−26	−78	−2.2
9	5′-d(GCG**4**AGC)-3′, **21**	9	*B*	67	−25	−73	−2.2
10	5′-d(GCG**4**AGC)-3′, **21**	4.5	*B*	66	−25	−73	−2.2
11	5′-d(GCG**4**AGC)-3′, **21**	26	*A*	66	−28	−83	−2.5
12	5′-d(GCG**4**AGC)-3′, **21**	18	*A*	68	−29	−87	−2.5
13	5′-d(GCG**4**AGC)-3′, **21**	9	*A*	68	−31	−90	−2.9
14	5′-d(GCG**4**AGC)-3′, **21**	4.5	*A*	71	−32	−90	−2.9
15	5′-d(GCGA**4**GC)-3′, **22**	4–26	*A*	60	−21	−62	−1.5
16	5′-d(GCG**44**GC)-3′, **23**	4–26	*A*	59	−23	−68	−2.0
17	5′-d(GCG**5**AGC)-3′, **24**	4–26	*A*	65	−23	−67	−2.0
18	5′-d(GCGA**5**GC)-3′, **25**	4–26	*A*	< 15	–	–	–
19	5′-d(GCG**55**GC)-3′, **26**	4–26	*A*	< 15	–	–	–
20	5′-d(GCG**6**AGC)-3′, **27**	4–26	*A*	67	−24	71	2.3
21	5′-d(GCGA**6**GC)-3′, **28**	4–26	*A*	< 15	–	–	–
22	5′-d(GCG**66**GC)-3′, **29**	4–26	*A*	< 15	–	–	–
23	5′-d(GCG**7**AGC)-3′, **30**	4–26	*A*	53	−22	−68	−1.1
24	5′-d(GCG**8**AGC)-3′, **31**	4–26	*A*	45	−33	−104	−0.9
25	5′-d(GC**9**AAGC)-3′, **32**	4–26	*A*	62	−26	−77	−2.0
26	5′-d(GC**10**AAGC)-3′, **33**	10	*A*	71	−25	−73	−2.6

[a]) The underlined oligonucleotide sequence marks the modification of the corresponding parent sequence. [b]) Buffer systems: *A*, 10 mM Na-cacodylate, 10 mM $MgCl_2$, 100 mM NaCl, pH 7; *B*, 0.1M NaCl; *C*, 1M NaCl, 1 mM EDTA, 10 mM Na_3PO_4, pH 7; *D*, 1 : 1 mixture of formamide/10 mM Na-cacodylate, 10 mM $MgCl_2$, 100 mM NaCl, pH 7; *E*, 20 mM Li_3PO_4, 50 mM KCl; *F*, 20 mM Li_3PO_4, 50 mM NaCl; *G*, 20 mM Li_3PO_4, 50 mM LiCl; H, 20 mM Li_3PO_4, 50 mM CsCl.

A striking decrease is, however, found when either a propane-1,3-diol (**7**) or a 2-deoxyribose (**8**) moiety are introduced into the minihairpin at position 4 (*Table 2*, *Entries 23* and *24*, resp.). In these cases, stabilization by stacking between residues 3 and 4 is fully omitted. Interestingly, the introduction of the flexible propanediol unit into the loop (*Entry 23*, T_m 53°) keeps the melting temperature comparably high, while the incorporation of the more rigid 2-deoxyribose (*Entry 24*) lowers the T_m value more significantly (45°). So, obviously the propanediol-containing minihairpin is better able

to adapt to the folding of the loop. These results indicate that stacking interactions between bases 3 and 4 do exist and force up the thermal stability of the minihairpin by roughly 15°, but the stability cannot be enhanced by the incorporation of better stackers than a purine ring system.

2.3.2. *Modifications of the dG·dA Sheared Base Pair of the Stem*. We also investigated the base-pairing properties of minihairpins modified at the $dG^3 \cdot dA^5$ base pair. In particular, compounds **4**–**6** were incorporated into position 5 (*Table 2*, *Entries 15*, *18*, and *21*, resp.) and the 8-aza-7-deazapurin-2-amine nucleoside **9** as well as 7-deaza-2′-deoxyguanosine (**10**) into position 3 (*Entries 25* and *26*, resp.). The incorporation of 1-deaza-2′-deoxyadenosine (**4**) into position 5 (*Entry 15*) as well as of compound **9** into position 3 (*Entry 25*) lowers the T_m value of the corresponding modified minihairpins only moderately. The motives **II** and **III** display the postulated base pairs $dG^3 \cdot \mathbf{4}^5$ and $\mathbf{9}^3 \cdot dA^5$, respectively. The decreased T_m values of the oligomers **22** (*Entry 15*) and **32** (*Entry 25*) compared to that of the parent minihairpin **1** can be attributed to the weaker H-bonding of the modified nucleosides **4** and **9** within the base pair motifs **II** and **III**.

Incorporation of either 7-deaza-2′-deoxyadenosine (**5**; motif **IV**) or 1,N^6-etheno-2′-deoxyadenosine (**6**) causes a complete denaturation of the hairpin structure that is not compensated by formation of a duplex structure due to too many mismatches (*Table 2*, *Entries 18* and *21*). Similar results are found for oligomers with two modified bases (*Entries 16*, *19*, and *22*); incorporation of two 1-deaza-2′-deoxyadenosine residues (*Entry 16*) still results in an oligomer forming a minihairpin (T_m 59°), while the incorporation of either two c^7A_d or εA_d residues (*Entries 19* and *22*) abolishes hairpin formation.

Finally, temperature-dependent UV spectra of the oligonucleotide **33** carrying a 7-deaza-2′-deoxyguanosine (**10**; $c^7G^3{}_d$) residue instead of dG^3 revealed a T_m value of 71° (*Entry 26*). This result established that in the case of the parent oligomer **1**, N(7) of dG^3 is not involved in the $dG^3 \cdot dA^5$ base pair (motif **V**) and makes a sheared base-pair motif (motif **I**) most plausible.

2.3.3. *Modified Nucleosides as Overhanging Units of the Minihairpin*. To enhance the stability, we synthesized the minihairpins **34**–**38** (*Table 3*, *Entries 27–34*), which carry an unpaired overhanging nucleoside, either dA (**3**), c^7A_d (**5**), εA_d (**6**), or a $(dT)_6$ tail (*Fig. 2*). T_m Measurements in 10 mM Na-cacodylate, 10 mM $MgCl_2$, and 0.1M NaCl (pH 7.0) reveal – except for the last example – T_m values above 80–85°. As such high T_m values are difficult to be measured, the melting experiments were performed in a 1:1 (*v*/*v*) mixture of formamide and the above-mentioned buffer.

According to *Table 3* (*Entries 27–34*), the dangling nucleotide unit enhances the T_m value of the parent oligomer (*Entry 34*) strongly (7–12°), whereby the amount of the T_m increase is dependent on the polarizability of the overhanging nucleobase. This confirms earlier results of our group and others [14] and is of practical importance as it enables a more effective protection of antisense oligonucleotides and primers for DNA amplification when oligomers such as **36** are tagged to their 5′-termini. A further advantage of the dangling nucleoside is the significant improvement of the cooperativity of the melting process. While for blunt-end hairpins the latter is often very low, therewith hampering the evaluation of thermodynamic data, hairpins with a nonpaired residue exhibit a pronounced *S*-shaped melting curve.

-

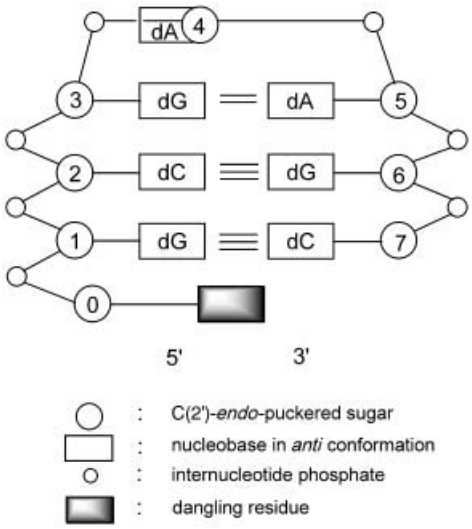

Fig. 2. *Schematic presentation of the minihairpin* **1** *with an unpaired overhanging nucleoside residue*

Table 3. T_m *Values and Thermodynamic Data of the Formation of the Parent Minihairpin* **1** *Carrying Various Nonpaired Overhangs*

Entry	Oligonucleotide	Conc. [μM]	Buffer[a])	T_m [°]	$\Delta H°$ [kcal/mol]	$\Delta S°$ [cal/(mol K)]	$\Delta G°_{310}$ [kcal/mol]
27	5′-d(**A**GCGAAGC)-3′, **34**	12	*D*	45	−21	−67	−0.6
28	5′-d(**5**GCGAAGC)-3′, **35**	12	*D*	45	−21	−65	−0.5
29	5′-d(**6**GCGAAGC)-3′, **36**	12	*D*	50	−23	−72	−0.9
30	5′-d(**T_6**GCGAAGC)-3′, **37**	10	*A*	74	−35	−102	−3.8
31	5′-d(**T_6A**GCGAAGC)-3′, **38**	10	*A*	73	−36	−105	−3.8
32	5′-d(**T_6**GCGAAGC)-3′, **37**	10	*D*	44	−25	−78	−0.6
33	5′-d(**T_6A**GCGAAGC)-3′, **38**	10	*D*	38	−29	−93	−0.1
34	5′-d(GCGAAGC)-3′, **1**	12	*D*	38	−19	−61	−0.04

[a]) For buffer systems, see *Table 2*, *Footnote b*.

Table 4 summarizes ^{1}H- and ^{31}P-NMR data of the minihairpin **1** as well as those of the oligonucleotide **34**; both data sets of compound **1** are in full agreement with data already published [15]. Tagging an overhanging dA^0 residue to the parent sequence causes relatively large chemical shift differences for the P-atom between dG^1 and dC^2 ($\Delta\delta(^{31}P) = +0.11$ ppm), while the other ^{31}P-NMR resonances are shifted to a much lesser extent ($\Delta\delta(^{31}P) < 0.05$ ppm) (*Fig. 3*). An analogous result is found upon comparison of the ^{1}H-NMR spectra; the largest chemical-shift differences between the H−C(8)/H−6 signals are found for the terminal residues dG^1 and dC^7 ($\Delta\delta(^1H) =$ 0.14–0.20 ppm). As already described for oligomer **1,** the ^{1}H-NMR spectrum of **34** also exhibits different H−C(1′)-signal shapes: those of dG^3, dA^4, and dA^5 are broad and not

Table 4. *Selected ^1H- and ^{31}P-NMR Chemical Shifts of the Parent Minihairpin* **1** *and of the Oligomer* **34** *in D_2O at 303 K*

Oligonucleotide	$\delta(^1H)$ [ppm]							
	dG^1 H–C(8)	dC^2 H–C(5), H–C(6)	dG^3 H–C(8)	dA^4 H–C(8), H–C(2)	dA^5 H–C(8), H–C(2)	dG^6 H–C(8)	dC^7 H–C(5), H–C(6)	dA^0 H–C(8), H–C(2)
5′-d($G^1C^2G^3A^4A^5G^6C^7$)-3′, **1**	8.00	5.07, 6.91	7.94	8.02, 8.00	7.91, 8.04	7.83	5.47, 7.29	–
5′-d($A^0G^1C^2G^3A^4A^5G^6C^7$)-3′, **34**	7.86	4.91, 6.89	7.95	8.02, 8.00	7.87, 8.05	7.84	5.40, 7.49	7.86, 7.97
Oligonucleotide	$\delta(^{31}P)$ [ppm]							
	$d(G^1pC^2)$	$d(C^2pG^3)$	$d(G^3pA^4)$	$d(A^4pA^5)$	$d(A^5pG^6)$	$d(G^6pC^7)$	$d(A^0pG^1)$	
5′-d($G^1C^2G^3A^4A^5G^6C^7$)-3′, **1**	−0.0070	−0.5932	−0.3219	−0.4349	−0.7633	+0.5448	–	
5′-d($A^0G^1C^2G^3A^4A^5G^6C^7$)-3′, **34**	+0.1060	−0.5937	−0.3680	−0.4532	−0.7535	+0.5758	−0.1759	

resolved (at 25°), while all other residues including the overhanging dA^0 give sharp peaks. This is probably due to a structural fluctuation in the loop region caused by wobbling of the dA^5 residue, while the overhanging dA^0 is stacked rigidly on the neighboring $dG^1 \cdot dC^7$ base pair.

2.3.4. *Influence of Sequence Variations on the Thermal Stability of the Minihairpin* **1**. Upon molecular-model building based on NMR analyses, *Wilson* and co-workers [16] found that the order 5′-d(GA)-3′ is crucial for the formation of a guanine · adenine sheared base pair of type **I**. The opposite sequence 5′-d(AG)-3′ can also form a base pair of type **I**, but the guanine(3)···adenine(4) stacking such as in **1** does no longer exist, and the duplex is severely distorted. Analogous results have been obtained for corresponding RNA duplexes.

To evidence this phenomenon on the DNA minihairpin **1**, the oligomer 5′-d(GCAAGGC) (**39**) was synthesized, and its T_m value was determined (*Table 5*, *Entry 35*). As can be seen, **39** exhibits a melting temperature of just *ca.* 40° and is thus destabilized by *ca.* 30°. Measurement of concentration-dependent T_m values of **39** reveal a sloped line so that antiparallel duplex formation with probably 4 $G_d \cdot C_d$ and 1 $G_d \cdot A_d$ base pairs, flanking a bulge loop, has to be considered. It is, however, worth to mention that the melting profiles of **39** at low concentration (< 1 A_{260} unit/ml) exhibit

Table 5. T_m *Values and Thermodynamic Data of the Formation of Sequence-Modified Minihairpins and Duplexes*

Entry	Oligonucleotide[a])	Conc. [μM]	Buffer[b])	T_m [°]	ΔH° [kcal/mol]	ΔS° [cal/Kmol]	ΔG°_{310} [kcal/mol]
35[c])	[5′-d(GCAAGGC)]$_2$, (**39**)$_2$	10	*A*	40	−31	−78	−6.9
36	5′-d(**A**GCAAGGC)-3′, **40**	10	*A*	52	−20	−62	−0.9
37	5′-d(GCGAAGA)-3′, **41**	10	*A*	*ca.* 60	–	–	–
38	5′-d(**A**GCGAAGC)-3′, **34**	5+5	*A*	21	−37	−148	8.3
	3′-d(CGCTTCG)-3′, **42**			74	−56	−180	0.2
39	5′-d(GCGAAGC)-3′, **1**	5+5	*A*	–	–	–	–
	3′-d(CGCTTCG)-5′, **42**						

[a]) The underlined oligonucleotide sequence marks the modification of the corresponding parent sequence. [b]) For buffer systems, see *Table 2*, *Footnote b.* [c]) Thermodynamic data are calculated from concentration-dependent T_m measurements.

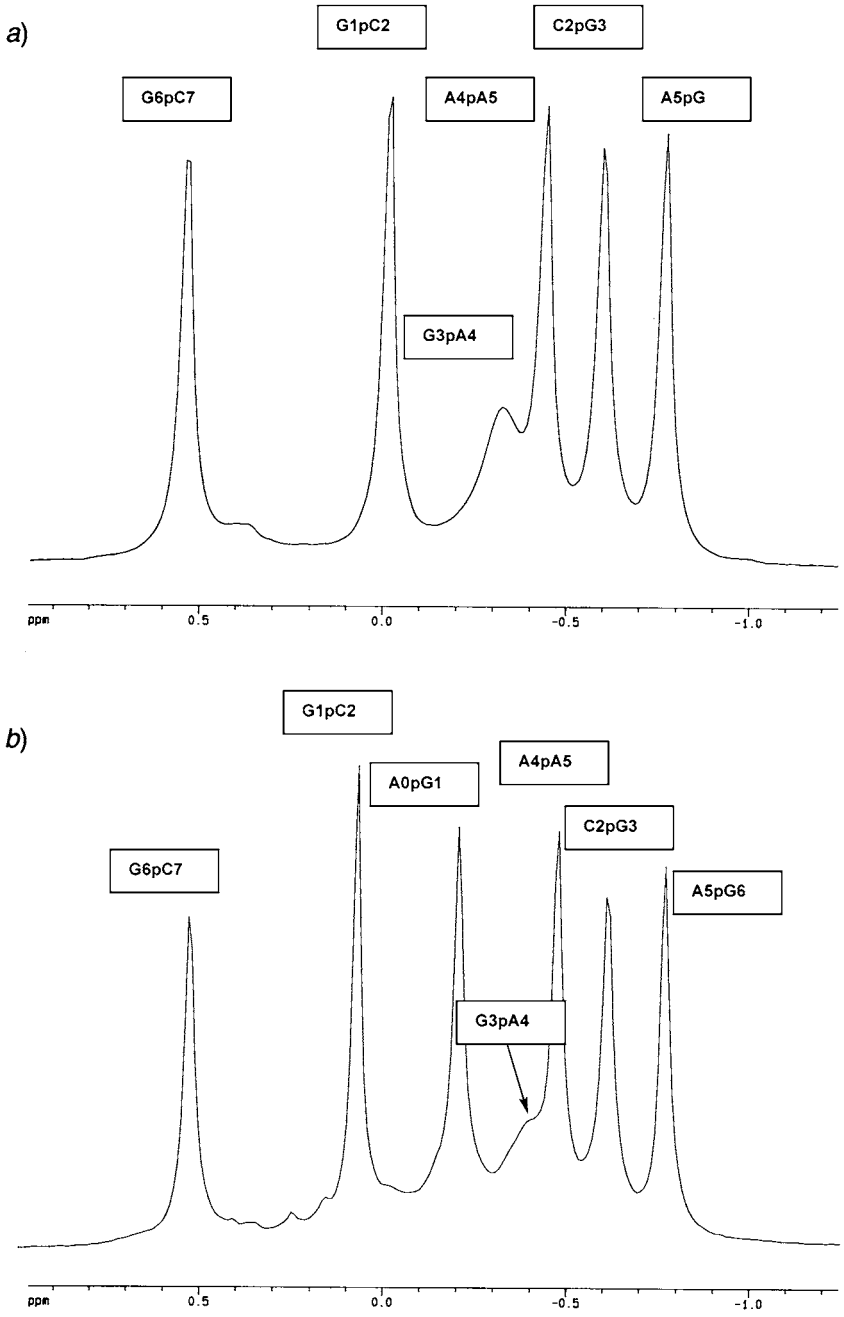

Fig. 3. *^{31}P-NMR Spectrum* (D_2O, 303 K) *of* a) *the minihairpin* **1** *and of* b) *the extended minihairpin* **34** *carrying an overhanging 5′-dA residue*

low cooperativity; calculation of the first derivative of these melting curves shows an only slightly distinct second transition at 55–60° (data not shown), which is concentration-independent and might indicate the presence of a hairpin being in equilibrium with the duplex. In this concern, it is interesting to mention that attachment of a nonpaired overhanging dA to the 5′-terminus of the oligomer **39** gives an oligomer **40** which is clearly a hairpin with a T_m value of 52° (ΔT_m (**40** – **39**) = 12°).

The oligomer 5′-d(GCGAAGA)-3′ (**41**) having a dG · dA base pair at the termini of the potential hairpin exhibits a melting profile with very low cooperativity from which no reliable data can be drawn (T_m *ca.* 60° ± 5°; *Table 5*, *Entry 37*). These results underline the crucial importance of the particular sequence motif for the minihairpin formation.

The obvious existence of a duplex structure as described above prompted us to investigate an equimolar mixture of the oligomer **1** and its opposite strand in antiparallel arrangement, *i.e.*, 5′-d(GCGAAGC)-3′ · 3′-d(CGCTTCG)-5′ (**1** · **42**). Up to 95°, no cooperative melting could be observed, a finding that lacks a meaningful explanation until now, because the first single strand forms a stable hairpin and the second one does not form any secondary structure. The situation becomes even more enigmatic when the first strand **1** is extended by a nonpaired dA residue (see **34** · **42**). In this case, a melting profile with two inflection points representing T_m values of *ca.* 21° and 74° are clearly observed (*Table 5*, *Entry 38*). This points to the coexistence of a duplex and a hairpin structure. The question why in the former case no secondary structure is formed remains, however, open.

2.4. *Aptamer-Minihairpin Fusions.* Next, we merged two thermostable structural elements, namely the minihairpin 5′-d(GCGAAGC)-3′ (**1**) and the aptamer 5′-d(GGTTGGTGTGGTTGG)-3′ (**2** = **46**), representing a triple hairpin formed by a G tetrade (*Fig. 1*,*b*), into the new secondary structure 5′-d(GGTTGGGCGAAGCGGTTGG)-3′ (**43**). This investigation was prompted by a publication of *Macaya* and co-workers [17] who selected (*SELEX*) a single-stranded DNA oligonucleotide ligand to the serine protease thrombin, which combined a quadruplex and a pending duplex structure (quadruplex/duplex molecule). In the same publication, the authors reported also on the bridging of the 5′- and 3′-ends of the duplex motif with either triethylene glycol or disulfide bonds; therewith they improved both, thrombin inhibitory activity as well as nuclease resistance in serum.

Concentration-dependent T_m measurements of **43** (at λ 240 nm, heating rate 0.5°/min, cooling rate 0.5°/min, 10–98°; 20 mM Li_3PO_4, 50 mM KCl; *Table 6*, *Entry 40*) implied two transitions with T_m values of 43 and 70° revealing the separate melting of the aptamer (43°) and of the minihairpin (70°). The first is 5° below the T_m value of the regular thrombin-binding aptamer **46** (T_m 48°), while the second is identical to that of the minihairpin **1** (mean T_m 70°) (*Fig. 4*, *Table 6)*. This implies a slight influence of the stable minihairpin structure on the more labile structure of the aptamer, but not *per se vice versa*. The formation of the aptamer, structure was verified by measuring the T_m value of the oligomer **43** in the presence of Li^+, Na^+, K^+, and Cs^+ ions. Indeed, a strong ion dependence of T_m was detected in such a way that neither the Li^+- nor the Cs^+-containing sample showed a melting point above 15° (*Table 6*, *Entries 42* and *43*), while the Na^+-containing sample exhibited T_m values of 40° and 70° (*Entry 41*; for the data in a K^+-containing buffer, see *Entry 40*) [18]. As the single aptamer exhibits a melting

Table 6. T_m *Values and Thermodynamic Data of the Formation of Minihairpin-Aptamer Constructs*

Entry	Oligonucleotide[a])	Conc. [μM]	Buffer[b])	T_m [°]	$\Delta H°$ [kcal/mol]	$\Delta S°$ [cal/Kmol]	$\Delta G°_{310}$ [kcal/mol]
40	5′d(GGTTGGGCGAAGCGGTTGG)-3′, **43**	5	*E*	43	−37	−117	−0.7
				70	−48	−139	−4.5
41	5′-d(GGTTGGGCGAAGCGGTTGG)-3′, **43**	5	*F*	40	−35	−113	−0.4
				70	−31	−90	−3.0
42	5′-d(GGTTGGGCGAAGCGGTTGG)-3′, **43**	5	*G*	–	–	–	–
43	5′-d(GGTTGGGCGAAGCGGTTGG)-3′, **43**	5	*H*	–	–	–	–
44	5′-d(GGTTGGCGAAGGGTTGG)-3′, **44**	5	*E*	46	−42	−132	−1.2
45	5′-d(GGTTGGGAAGGTTGG)-3′, **45**	5	*E*	41	−34	−109	−0.4
46	5′-d(GGTTGGTGTGGTTGG)-3′, **46** (= **2**)	5	*E*	48	−45	−142	−1.5
47	5′-d(GGTTGGT**10**TGGTTGG)-3′, **47**	5	*E*	45	−37	−117	−0.7
48	5′-d(GGTTGGTTGGTTGG)-3′, **48**	5	*E*	–	–	–	–
49	5′-d(GGTTTGGTGTGGTTGG)-3′, **49**	5	*E*	48	−48	−150	−1.6
50	5′-d(GGTTGGTGTGGTTTGG)-3′, **50**	5	*E*	48	−45	−142	−1.5
51	5′-d(GCGAAGC)-3′, **1**	5	*E*	71	−29	−83	−2.8

[a]) The underlined oligonucleotide sequence marks the modification of the corresponding parent sequence. [b]) For buffer systems, see *Table 2*, *Footnote b*.

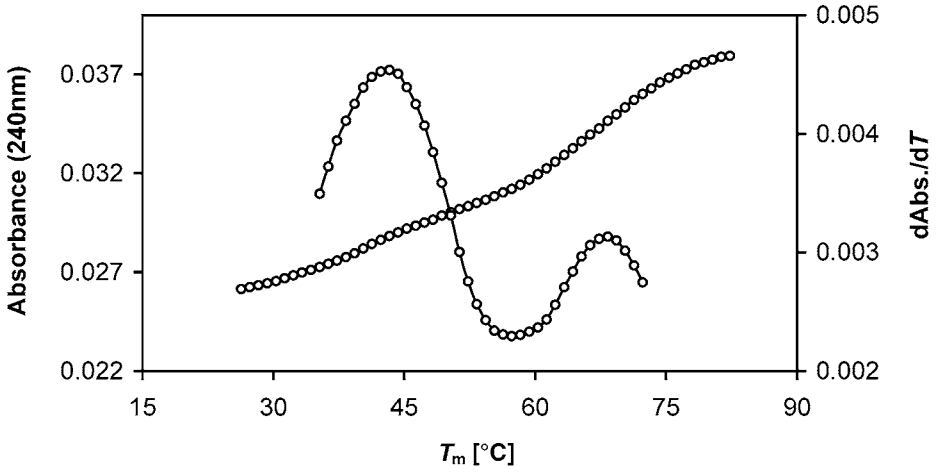

Fig. 4. *Melting profile and first derivative thereof for the oligonucleotide 5′-d(GGTTGGGCGAAGCGGTTGG)-3′* (**43**) *in 20 mM Li_3PO_4, 50 mM KCl* (pH 7). Oligomer concentration, 5 μM; for details, see *Exper. Part*.

temperature of *ca.* 20° in the presence of Na^+-ions, the conclusion can be drawn that the minihairpin forces the aptamer to form even under nonoptimal buffer conditions.

Comparison of the thermodynamic data ($\Delta H°$, $\Delta S°$) of secondary-structure formation for both parts of the aptamer–minihairpin construct **43** with those of the two separated oligonucleotides **1** (minihairpin) and **46** (aptamer) discloses an interesting feature (*Table 6*, *Entries 40*, *46*, and *51*, resp.): the corresponding data show a significant dissipation when going from the fused oligonucleotide **43** to the

single oligomers **1** and **46** or, in other words, the difference of the ΔH° and particularly of the ΔS° values is smaller in case of the construct **43** than for the separated oligomers. This points to a mutual structural influence of the two structures within the same oligonucleotide.

Truncation of the core sequence to 5′-d(CGAAG)-3′ (→ **44**) leads to a slight increase of the lower T_m value (46°) of the resulting oligomer; the upper transition (melting of a minihairpin) can no longer be detected (*Table 6*, *Entry 44*). Further truncation to 5′-d(GAA)-3′ (→ **45**) gives also a monophasic transition with a T_m value of 41° (*Entry 45*). An innermost 3-base loop seems to be the minimum length which is tolerated; a reduction to the 2-base loop d(TT) (→ **48**) abolishes the formation of any secondary structure (*Entry 48*) reflecting the strain on the G-tetrade involved in decreasing the central-loop size. The replacement of the central dG of the d(TGT) loop by compound **10** (→ **47**) reduces the T_m value of the aptamer only slightly ($\Delta T_m = -3°$; *Entry 47*), reflecting the lower stacking of the 7-deazapurine base compared to guanine.

Inspection of the oligonucleotide sequences **43** – **45** discloses various possibilities of secondary structures the oligomers might adopt. The single strand **43** can be arranged in two ways maintaining a chair-like structure (*Fig. 5*, motives **VI** and **X**). Motif **VI** retains

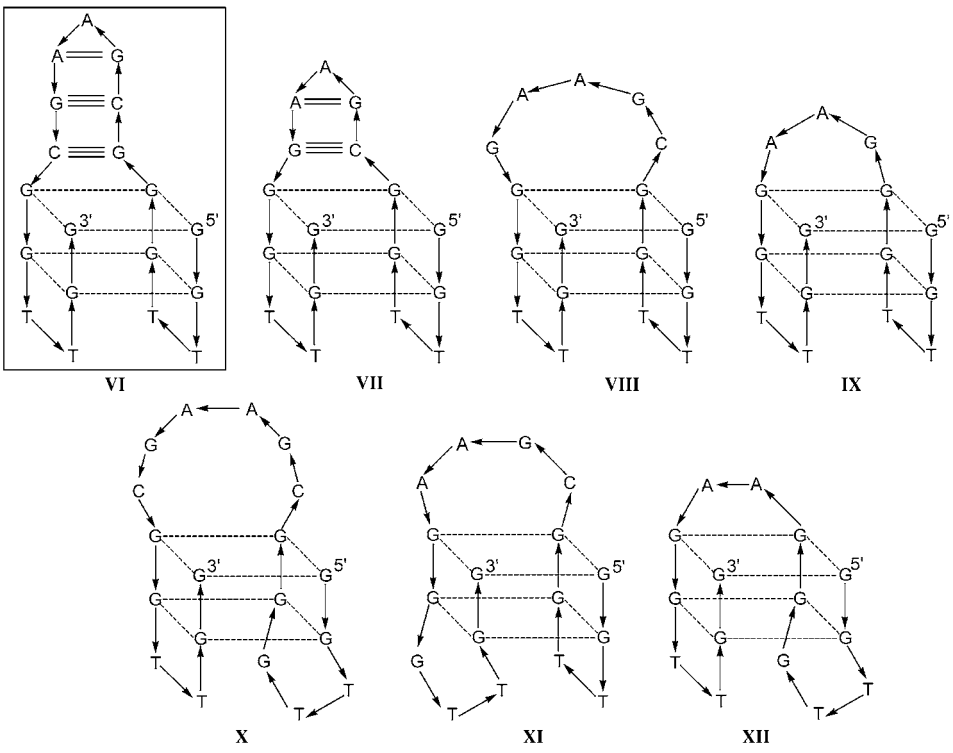

Fig. 5. *Schematic presentation of the aptamer-minihairpin construct* **43** *as well as of the various conceivable chair-like secondary structures of the oligomers* **43** – **45**

the two d(TT) loops but contains a seven-base minihairpin in the center. Motif **X** includes the 5′-terminal dG of the minihairpin (position 7 of **43**) in the formation of the G quartet. This results in an unsymmetric chair with a three-base loop on the 5′-side (5′-d(TTG)-3′), a two-base loop on the 3′-side (d(TT)), and a six-base loop in the center (5′-d(CGAAGC)-3′). Also this secondary structure can be ruled out, because such a structure should show only a monophasic melting curve.

In the case of the oligomer **44**, the situation is similar: besides the topologically symmetric chairs with either a truncated minihairpin (*Fig. 5*, motif **VII**) or an unpaired five-base loop (motif **VIII**), a frame shift of the G-tetrade-forming d(GG) units results again in an unsymmetric chair (motif **XI**). In this case, however, the d(TT) loop is located on the 5′-side, while the three-base loop 5′-d(GTT)-3′ is positioned on the 3′-side; the central loop consists of the tetramer 5′-d(CGAA)-3′. As this oligomer **44** exhibits only a monophasic melting profile with a T_m value that corresponds to that of the aptamer, a clear decision between the possible structures **VII**, **VIII**, and **XI** cannot be made. Least, also oligomer **45** might exist (or fluctuate) in two chair-like structural variants – the topologically symmetric chair (motif **IX**) or the unsymmetric motif **XII**, again with the d(TT) loop on the 3′-side as for oligomer **43**.

The reader might imagine the various structures as rocking chairs with differential backrest size, which are either standing straight or which are tilted either to the left- or to the right-hand side. Moreover, other conformations, *e.g.*, backwards-tilted and therewith no longer upright backrest loops are conceivable. Additionally, basket-like secondary structures and parallel or antiparallel arranged duplex structures are principally conceivable. The latters, however, can be ruled out due to the concentration independence of the T_m values of the oligomers. Which of the structures the oligomers **43**–**45** do ultimately (predominantly) form is difficult to decide. *Shafer* and co-workers [19] pointed out that both sequence and length of the two loops forming the runners of the rocking chair are of minor importance for the thermal stability of the aptamer. This could be verified by measuring the T_m values of the oligomers **49** and **50** (*Table 6*, *Entries 49* and *50*). Sequence and size of the central loop, however, is of critical importance: extension from three to four bases ($d(T)_4$) or truncation from three to two bases ($d(T)_2$) lowers the T_m value of the aptamer by 12 and 25°, respectively. The latter result is confirmed by our finding that the oligomer **48** exhibits no melting point above 20°.

The results of *Shafer* supports the finding that in the case of oligomer **43**, the inner core, representing the minihairpin sequence, is indeed fully paired and consists of a seven-base (motif **VI**, *Fig. 5*) and not of a six-base moiety (motif **X**) being just looped out. The melting profile establishes the existence of both the G-tetrade and a hairpin heptamer within the same molecule (motif **VI**).

For oligomer **44**, only one transition is observed, but a clear decision about the structure (motif **VII**, **VIII**, or **XI**, *Fig. 5*) cannot be made. For oligonucleotide **45**, we are in favor of the structural motif **IX** with a three-base central loop, because the alternative structure (motif **XII**) having a d(AA) central loop should possess a significantly lower thermal stability as the one observed (T_m 41°).

3. Conclusion. – The oligodeoxynucleotide 5′-d(GCGAAGC)-3′ (**1**) adopts a very particular minihairpin structure, which seems not to be open for many structural

variations. Inversion of the $dG^3 \cdot dA^5$ base pair to a $dA^3 \cdot dG^5$ pair decreases the thermal stability drastically. However, the results indicate that structural modifications by using base-modified nucleosides are accepted, when the modified residues do not destroy the H-bonding network of the hairpin structure. Decreasing the stacking interaction of the fourth with the third base results in a T_m decrease of the minihairpin **1** compared to that containing the propane-1,3-diol residue at position 4, indicating that such minihairpins are rather stable, even when a base stack between the stem and the loop region is not existing. Moreover, 1-deazapurines, which cannot form *Watson–Crick* base pairs, are able to take part in a *Hoogsteen* interaction thereby forming stable hairpins. This modification will stabilize the hairpin over that of a duplex in the presence of the opposite strand. Also, the presence of the opposite strand of the oligomer **1** leads to the abolishment of hairpin formation of **1**. Insertion of the hairpin-forming sequence **1** (T_m 70°) into the position of the central loop of the thrombin-binding aptamer **46** (T_m 48°) yields 5′-d(GGTTGGGCGAAGCGGTTGG)-3′ (**43**). This oligonucleotide construct is able to form both a G-tetrade and a joined minihairpin structure. According to the T_m data, the minihairpin induces a small structural change in the aptamer section. Such structural effects within an oligonucleotide are of considerable interest and were already observed on RNAs. Investigations of the thrombin binding and possible allosteric effects [20] occurring on the aptamer are underway.

We gratefully acknowledge excellent technical assistance by Mrs. *Elisabeth Feiling* as well as Dr. *J. Shen* for preparing the oligomers **33** and **39**. We also thank the *Deutsche Forschungsgemeinschaft* (Graduiertenkolleg Nr. 612 'Molekulare Physiologie: Wechselwirkungen zwischen zellulären Nanostrukturen') (*F. S.* and *A. J.*) and the *Roche Diagnostics GmbH*, Penzberg, Germany, for financial support.

Experimental Part

General. Oligonucleotide syntheses were performed on a DNA/RNA synthesizer, model *392* (*Applied Biosystems*, Weiterstadt, Germany) with commercially available phosphoramidites of the regular 2′-deoxynucleosides as well as with the modified phosphoramidites **13**–**15**, which are also purchasable. The phosphoramidites **11** [22], **12** [23], **16** [24], and **17** [25] were prepared in our laboratory. All oligonucleotides containing 1-deaza-2′-deoxyadenosine (**4**) or 1,N^6-etheno-2′-deoxyadenosine (**6**) were synthesized with *t*-butylphenoxyacetyl (tac)-protected phosphoramidites of the canonical nucleoside building blocks. These oligomers were deprotected by the 'fast-deprotection' procedure (2 h, 25% aq. NH_3 soln.). UV Spectra: *U-3000*- or *U-3200*-UV/VIS photospectrometers (*Hitachi*, Japan). MALDI-TOF-MS: *Biflex-III* instrument (*Bruker Daltronik GmbH*, Leipzig, Germany) in the reflector mode; for details see [21].

HPLC Purification of Oligonucleotides. The purification of oligonucleotides was performed on an *RP-18-LiChrosorb* HPLC column (10 × 250 mm) by using a *Merck-Hitachi* control unit (model *655 A-12*) with a UV monitor (model *655 A*) and an integrator (model *D 2500*). Solvent systems: *A*, 100% MeCN; *B*, 5% MeCN in 0.1M (Et_3NH)OAc buffer (pH 7); *C*, 100% H_2O; *D*, MeOH/H_2O 3 : 2 (*v*/*v*). The following solvent gradients were used: 1. Purification of oligomers synthesized in the 'DMT-on' mode: 3 min 15% *A* in *B*, 7 min 15–40% *A* in *B*, 5 min 40% *A* in *B*, 5 min 40–15% *A* in *B*, 5 min 15% *A* in *B*, flow 0.8 ml/min. 2. Purification of oligomers synthesized in the 'DMT-off' mode: 15 min 0–10% *A* in *B*, 5 min 10% *A* in *B*, 5 min 15–0% *A* in *B*, 5 min 0% *A* in *B*; flow 1 ml/min. 3. Purification of oligomers after manual detritylation: 20 min 0–15% *A* in *B*, 5 min 15% *A* in *B*, 5 min 15–0% *A* in *B*, 5 min 0% *A* in *B*, flow 1 ml/min. Desalting: 15 min *C*, 10 min *D*, flow 0.6 ml/min.

The enzymatic hydrolysis of the unmodified oligomers with snake-venom phosphodiesterase (EC 3.1.15.1, *Crotallus adamanteus*) and alkaline phosphatase (EC 3.1.3.1, *E. coli*) was carried out as described [26]. The mixture was analyzed by reversed-phase HPLC (*RP-18*, solvent system III). Quantification of the resulting nucleosides was made on the basis of the peak areas which were divided by the extinction coefficients of the nucleoside constituents at λ 260 nm.

T_m *Measurements.* The thermal dissociation/association of the oligomers was measured by temp.-dependent UV melting profiles (220–350 nm) with a *Cary-1E*-UV/VIS spectrophotometer (*Varian*, Australia) equipped with a *Cary* thermoelectrical controller; the actual temp. was measured in the reference cell with a Pt-100 resistor. T_m Values were determined at that wavelength of the UV spectra where the difference of the absorbances at the highest and the lowest temp. was most pronounced. The thermodynamic data of duplex formation were calculated by curve fitting to a two-state-model using the program MeltWin [27] or by concentration-dependent T_m measurements. The data of oligonucleotides showing two transitions were evaluated by separate fitting of the melting profiles either in the high- or in the low-temp. range.

REFERENCES

[1] A. B. Steel, R. L. Levicky, T. M. Herne, M. J. Tarlov, *Biophys. J.* **2000**, *79*, 975.

[2] W. Saenger, 'Principles of Nucleic Acid Structure', Springer Verlag, New York, Berlin, Heidelberg, 1984, p. 298 f.

[3] S.-H. Chou, K.-H. Chin, A. H.-W. Wang, *Nucleic Acids Res.* **2003**, *31*, 2461.

[4] T. Batey, R. P. Rambo, L. Lucast, B. Rha, J. A. Doudna, *Science (Washington, D.C.)* **2000**, *287*, 1232; M. Orita, F. Nishikawa, T. Shimayama, K. Taira, Y. Endo, S. Nishikawa, *Nucleic Acids Res.* **1993**, *21*, 5670; J. P. Simorre, P. Legault, A. B. Hangar, P. Michiels, A. Pardi, *Biochemistry* **1997**, *36*, 518; J. E. Wedekind, D. B. McKay, *Ann. Rev. Biophys. Biomol Struct.* **1998**, *27*, 475; P. Fan, A. K. Suri, R. Fiala, D. Live, D. J. Patel, *J. Mol. Biol.* **1996**, *258*, 480; J. Santa Lucia Jr., D. H. Turner, *Biochemistry* **1993**, *32*, 12612; J. H. Cate, A. R. Gooding, E. Podell, K. Zhou, B. L. Golden, C. E. Kundrot, T. R. Cech, J. A. Doudna, *Science (Washington, D.C.)* **1996**, *273*, 1678.

[5] S.-H. Shou, K.-H. Chin, A. H.-J. Wang, *Nucleic Acids Res.* **2003**, *31*, 2461, and refs. cit. therein; G. B. Prive, U. Heinemann, S. Chandrasegaran, L.-S. Kan, M. L. Kopka, R. E. Dickerson, *Science (Washington, D.C.)* **1987**, *238*, 498; X. Gao, D. J. Patel, *J. Am. Chem. Soc.* **1988**, *110*, 5178; T. Brown, W. N. Hunter, G. Kneale, O. Kennard, *Proc. Natl. Acad. Sci. USA* **1986**, *83*, 2402; G. A. Leonard, E. D. Booth, T. Brown, *Nucleic Acids Res.* **1990**, *18*, 5617.

[6] P. J. Barr, R. M. Thayer, P. Laybourn, R. C. Najarian, F. Seela, D. R. Tolan, *BioTechniques* **1986**, *4*, 428; S. Mizusawa, S. Nishimura, F. Seela, *Nucleic Acids Res.* **1986**, *14*, 1319.

[7] I. M. Khan, J. M. Coulson, *Nucleic Acids Res.* **1993**, *21*, 2957.

[8] H. Han, L. H. Hurley, *Trends Pharmacol. Sci* **2003**, *21*, 136, and refs. cit. therein; V. Dapic, V. Abdomerovic, R. Marrington, J. Peberdy, A. Rodger, J. O. Trent, P. J. Bates, *Nucleic Acids Res.* **2003**, *31*, 2097, and refs. cit. therein.

[9] L. C. Bock, L. C. Griffin, J. A. Latham, E. H. Vermaas, J. J. Toole, *Nature (London)* **1992**, *355*, 564.

[10] I. Hirao, G. Kawai, S. Yoshizawa, Y. Nishimura, Y. Ishido, K. Watanabe, K. Miura, *Nucleic Acids Res.* **1994**, *22*, 576; S. Yoshizawa, G. Kawai, K. Watanabe, K. Miura, I. Hirao, *Biochemistry* **1997**, *36*, 4761; I. Hirao, Y. Nishimura, T. Naraoka, K. Watanabe, Y. Arata, K. Miura, *Nucleic Acids Res.* **1989**, *17*, 2223; I. Hirao, Y. Nishimura, Y. Tagawa, K. Watanabe, K. Miura, *Nucleic Acids Res.* **1992,** *20*, 3891.

[11] I. Hirao, M. Ihida, K. Watanabe, K. Miura, *Biochim. Biophys. Acta* **1990,** *1087,* 199.

[12] N. Ramzaeva, H. Rosemeyer, P. Leonard, K. Mühlegger, F. Bergmann, H. von der Eltz, F. Seela, *Helv. Chim. Acta* **2000**, *83*, 1108.

[13] 'ChemSketch', V. 4.55, Advanced Chemistry Developments, Inc., Toronto, Canada; http://www.acdlabs.-com.

[14] H. Rosemeyer, F. Seela, *J. Chem. Soc., Perkin Trans. 2* **2002**, 746.

[15] S. Yoshizawa, G. Kawai, K. Watanabe, K. Miura, I. Hirao, *Biochemistry* **1997**, *36,* 4761; I. Hirao, G. Kawai, S. Yoshizawa, Y. Nihimura, Y. Ishido, K. Watanabe, K. Miura, *Nucleic Acids Res.* **1994**, *22*, 576.

[16] K. L. Greene, R. L. Jones, Y. Li, H. Robinson, A. H.-J. Wang, G. Zon, W. D. Wilson, *Biochemistry* **1994**, *33*, 1053.

[17] R. F. Macaya, J. A. Waldron, B. A. Beutel, H. Gao, M. E. Joesten, M. Yang, R. Patel, A. H. Bertelsen, A. F. Cook, *Biochemistry* **1995**, *34*, 4478.

[18] N. Jing, R. F. Rando, Y. Pommier, M. E. Hogan, *Biochemistry* **1997**, *36*, 12498.

[19] I. Smirnov, R. H. Shafer, *Biochemistry* **2000**, *39*, 1462.

[20] N. Sudarsan, J. E. Barrick, R. R. Breaker, *RNA* **2003**, *9*, 644; M. Mandal, B. Boese, J. E. Barrick, W. C. Winkler, R. R. Breaker, *Cell* **2003**, *113*, 577.

[21] H. Rosemeyer, F. Seela, *J. Chem. Soc., Perkin Trans. 2* **2002**, 746.

[22] F. Seela, T. Wenzel, *Helv. Chim. Acta* **1994**, *77*, 1485; F. Seela, T. Wenzel, H. Debelak, *Nucleosides Nucleotides* **1995**, *14*, 957; H. Debelak, Ph.D. Thesis, University of Osnabrück, 2002.
[23] F. Seela, A. Kehne, *Biochemistry* **1987**, *26*, 2232; F. Seela, H. Berg, H. Rosemeyer, *Biochemistry* **1989**, *28*, 6193.
[24] F. Seela, G. Becher, *Helv. Chim. Acta.* **2000**, *83*, 928.
[25] F. Seela, H. Driller, *Nucleic Acids Res.* **1989**, *17*, 901.
[26] F. Ssela, S. Lampe, *Helv. Chim. Acta* **1991**, *74*, 1790.
[27] J. A. McDowell, D. H. Turner, *Biochemistry* **1996**, *35*, 14077.

Received September 15, 2003